ภาคผนวก ก

ตารางแสดงความก้าวหน้าของโครงการ ณ ช่วงรายงานเมื่อเทียบกับแผนการดำเนินงานทั้งโครงการ

รายละเอียดกิจกรรม	ความก้าวหน้าของโครงการ / เดือน											
	1	2	3	4	5	6	7	8	9	10	11	12
1. หาข้อมูล ด้านความดัน, ความต่างศักย์ และขนาดของ และออกแบบอุปกรณ์ไดอิเลคโทรโฟริติค												
2. สร้างแบบจำลองในโปรแกรม Comsol												
3. ศึกษาพฤติกรรมของสนามไฟฟ้า การไหลของของเหลว และแรงไดอิเลคโทรโฟริติคที่ถูกสร้างบริเวณ block area												
4. ออกแบบระยะห่างระหว่าง block เพื่อให้มีขนาดแรงไดอิเลคโทรโฟริติคมากที่สุด												
5. ออกแบบความกว้างของ block เพื่อให้มีขนาดแรงไดอิเลคโทรโฟริติคมากที่สุด												
7. สรุปผล จัดทำรายงานฉบับสมบูรณ์ และเผยแพร่												

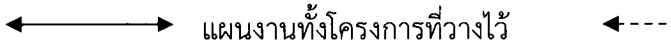

หมายเหตุ ข้อมูลรายละเอียดกิจกรรม แผนงาน/รูปแบบตาราง เปลี่ยนแปลง หรือปรับได้ตามความเหมาะสม

ภาคผนวก ข

สรุปค่าใช้จ่ายการดำเนินงานโครงการวิจัย
แบบรายงานการใช้จ่ายเงินโครงการวิจัย
สถาบันเทคโนโลยีพระจอมเกล้าเจ้าคุณทหารลาดกระบัง
รายงานฉบับสมบูรณ์ ประจำปีงบประมาณ 2556

☐ แหล่งงบประมาณแผ่นดิน (แบบปกติ) ☑ แหล่งเงินรายได้

ชื่อโครงการ (ภาษาไทย) การวิเคราะห์เชิงตัวเลขของการเคลื่อนที่ของอนุภาคระดับไมโครมิเตอร์ ภายใต้อิทธิพลของกระแสไฟฟ้าและความดันในอุปกรณ์ไดอิเลคโทรโฟริติค

(ภาษาอังกฤษ) Numerical analysis of microparticle motion under combined hydrodynamics and electrokinetics in insulator-based dielectrophoretic devices

ชื่อ-สกุลหัวหน้าโครงการวิจัยผู้รับทุน/ผู้วิจัย (อ./ดร./ผศ./รศ./ศ.) ดร.ณัฐวุฒิ หลิ่วพิริยะวงศ์

รายงานในช่วงตั้งแต่วันที่ 1/ต.ค./56 ถึงวันที่ 31/มิ.ย./57

ระยะเวลาดำเนินการ 1 ปี - เดือน ตั้งแต่วันที่ 1/ต.ค./56 ถึงวันที่ 30/ก.ย./57

ข้อมูลการรายงานค่าใช้จ่ายงบประมาณโครงการวิจัย

1. การเบิกจ่ายงบประมาณ (กรณีการจ่ายเงินถ้าจ่ายงวดเดียวให้ลบข้อที่ไม่เกี่ยวข้องออก)

งวดที่ 1 60,000 บาท 100 % วันที่ได้รับอนุมัติให้เบิกจ่ายเงิน (ป/ด/ว) 16/01/57

2. สรุปงบประมาณค่าใช้จ่ายที่ใช้นับตั้งแต่เริ่มทำการวิจัยถึงปัจจุบัน (จำแนกตามหมวดค่าใช้จ่าย)

หมวดค่าใช้จ่าย	งบประมาณรวมทั้งโครงการ	ค่าใช้จ่าย (บาท)	คงเหลือ (หรือเกิน)
งบบุคลากร :ค่าจ้างชั่วคราว	-	-	-
งบดำเนินงาน			
ค่าตอบแทน	-	-	-
ค่าใช้สอย	40,000	-	-
ค่าวัสดุ	20,000	60,000	ได้ดำเนินการส่งเอกสารทางการเงินเป็นที่เรียบร้อยแล้ว
ค่าสาธารณูปโภค	-	-	-
งบลงทุน: ค่าครุภัณฑ์	-	-	-
รวม	60,000	60,000	0

.....
(ดร.ณัฐวุฒิ หลิ่วพิริยะวงศ์)
ลงนามหัวหน้าโครงการวิจัยผู้รับทุน
...../...../.....

.....
(.....)
ลงนามเจ้าหน้าที่การเงิน/เจ้าหน้าที่ที่เกี่ยวข้อง
...../...../.....

ภาคผนวก ค

วารสารที่ได้ตีพิมพ์ จำนวน 1 วารสาร

1. Lewpiriyawong, N., and Yang, C., *Continuous Separation of Multiple Particles by Size and Type Using Insulator-Induced Dielectrophoresis in a Modified H-filter,* Electrophoresis, 2014. 35: p. 714-720.

Nuttawut Lewpiriyawong[1]
Chun Yang[2]

[1]Department of Mechanical Engineering, King Mongkut's Institute of Technology Ladkrabang, Bangkok, Thailand
[2]School of Mechanical and Aerospace Engineering, Nanyang Technological University, Singapore

Received September 5, 2013
Revised November 18, 2013
Accepted November 30, 2013

Research Article

Continuous separation of multiple particles by negative and positive dielectrophoresis in a modified H-filter

The article presents a new application of the modified H-filter with insulating rectangular blocks using negative and positive DEP for separation of multiple particles in a continuous pressure-driven flow. The multiple insulating blocks fabricated along the main channel induce spatially nonuniform electric fields which exert differential repulsive (negative) or attractive (positive) DEP forces on particles, depending on the size and the polarizability of particles relative to their suspending medium. As a result, particles of different sizes and polarizability can be separated into different outlets of the H-filter. Numerical simulations are also performed to analyze the effects of block gap and width on electric field distribution and DEP force characteristics near the insulating blocks so as to provide design guidelines for optimal structural dimensions of the microfluidic device. The device performance is demonstrated by separating a three-sized particles mixture, including 2 μm fluorescent particles with an attractive DEP force and both 5 and 10 μm nonfluorescent particles with differential repulsive DEP forces. High separation rate of 99% is successfully achieved.

Keywords:
Continuous separation of multiple particles / Insulator-based dielectrophoresis / Modified H-filter
DOI 10.1002/elps.201300429

Additional supporting information may be found in the online version of this article at the publisher's web-site

1 Introduction

The ability to discriminate multiple target cells of different sizes and types from complex biosamples (e.g. blood) is an important issue in chemical and biomedical applications. DEP is a promising separation technique broadly used for differentiating target cells in microfluidics [1]. The mechanism of DEP separation is based on relative electric polarizability between the cells and their suspending medium in a nonuniform electric field. In other words, under an applied nonuniform electric field, two types of cells possessing different polarizabilities suspended in a liquid medium can be separated by positive and negative DEP (pDEP and nDEP).

In microfluidic DEP devices, a nonuniform electric field can be created by applying either AC voltage over metallic electrodes deposited on a channel substrate or DC voltage across reservoirs connecting a microfluidic insulating channel with variation in geometric structure. In the literature, various kinds of DEP electrodes have been reported, including planar metallic or indium tin oxide (ITO) electrodes [2, 3], 3D electrodes (made of gold [4], copper [5, 6], Si [7–9], SU-8 [10, 11]), liquid electrodes [12] and recently developed 3D composite conductive PDMS electrodes [13–15], and metal alloy microspheres [16, 17]. On the other hand, DC insulator-based DEP (DC-iDEP) devices usually involve insulating posts or blocks embedded in microfluidic channels. The presence of geometric variation can cause a change of electrical current density around insulating posts, giving rise to a nonuniform electric field for generating a DC-DEP force.

Unlike electrode-based DEP, iDEP offers numerous advantages such as no need of fabricated complex metallic electrodes, less fouling issues, mechanical robustness, chemical inert, and biocompatibility [18]. Hence, DC-iDEP devices have broadly been employed to separate binary target samples either by size or by type such as microparticles of two different sizes [19–21], live and dead *Bacillus subtilis* [22], *Escherichia coli* from *B. subtilis* in water [23], and *B. subtilis* from 200 nm particles [24] as well as to manipulate proteins [25]. In addition to

Correspondence: Professor Chun Yang, School of Mechanical and Aerospace Engineering, Nanyang Technological University, 50 Nanyang Avenue, Singapore 639798
E-mail: mcyang@ntu.edu.sg
Fax: +65-6792-4062

Abbreviations: CM, Clausius–Mossotti; **iDEP**, insulator-based DEP; **nDEP**, negative DEP; **pDEP**, positive DEP

Colour Online: See the article online to view Figs. 1–3 in colour.

DC electric field, a DC-offset AC electric field has actively been employed to induce DEP force near insulating constrictions or microstructures for transporting, sorting, separation, and focusing of binary mixtures of microparticles [26–29]. The DEP-based applications are not limited to the binary particle separation, and they have been successfully extended to the separation of more complex samples such as multiple bacterial target cell types using DEP tags [30]. However, an examination of the current literature studies shows that the iDEP technology for separating multiple particles has not been established [31–33]. To our best knowledge for separation of multiple particles in a continuous flow, no study has been reported to develop an AC insulator-based DEP (AC-iDEP) device using nDEP and pDEP and guidelines for designing multiple insulating blocks.

In this work, we introduce a modified H-filter design that incorporates insulating rectangular blocks to generate AC-DEP forces for continuous separation of multiple particles by nDEP and pDEP. The commercially available microfluidic H-filter developed by University of Washington offers continuous extraction and separation of analytes on the basis of analytes mass diffusion as a driving force [34]. However, the separation function of this device suffers low efficiency and can even fail for large-sized particles/cells whose mass diffusivity is very low. The modification of H-filter utilizing AC-iDEP allows for introducing a lateral DEP force to manipulate particles traversally. In addition, using COMSOL Multiphysics software, we numerically analyze the effects of block gap and width on electric field distribution and DEP force characteristics near insulating blocks such that optimal geometric dimensions of insulating blocks in the modified H-filter are selected in the device design. The device is demonstrated by separating a three-sized particles mixture in a continuous pressure-driven flow.

2 Materials and methods

2.1 DEP theory

DEP is referred to as the motion of a polarized dielectric particle suspended in a dielectric medium under an applied nonuniform electric field, and it is based on a physical phenomenon of electrical polarization effects [35]. Based on the dipole moment method, the time-average DEP force exerting on a spherical particle of radius a is expressed as [35]

$$\left\langle \vec{F}_{\mathrm{DEP}} \right\rangle = 2\pi\varepsilon_m a^3 \mathrm{Re}\left[\underline{f}_{\mathrm{CM}}(\omega)\right] \nabla \left|\vec{E}_{\mathrm{rms}}\right|^2, \tag{1}$$

where $\langle\rangle$ denotes the time-average operation, ε_m is the medium permittivity, and $\nabla|\vec{E}_{\mathrm{rms}}|^2$ represents the gradient of the square of the root-mean-square electric field. $\underline{f}_{\mathrm{CM}}(\omega) = (\underline{\varepsilon}_p - \underline{\varepsilon}_m)/(\underline{\varepsilon}_p + 2\underline{\varepsilon}_m)$ is the complex Clausius–Mossotti (CM) with $\mathrm{Re}[\underline{f}_{\mathrm{CM}}(\omega)]$ being its real part ranging from -0.5 to $+1$. $\underline{\varepsilon}_p$ and $\underline{\varepsilon}_m$ are the complex permittivity of the particle and the suspending medium, respectively. $\underline{\varepsilon} = \varepsilon - i\sigma/\omega$ is the complex permittivity, where ε and σ are, respectively, the electrical permittivity and conductivity, $i = \sqrt{-1}$, and $\omega = 2\pi f$ is the radian frequency of the electric field. When the particle is more polarizable than its suspending medium, one has $\mathrm{Re}[\underline{f}_{\mathrm{CM}}(\omega)] > 0$ indicating a pDEP force to attract the particle from low to high electric field regions. Conversely, when the suspending medium is more polarizable than the particle, one has $\mathrm{Re}[\underline{f}_{\mathrm{CM}}(\omega)] < 0$, suggesting an nDEP force to repel the particle from high to low electric field regions.

The CM factor can be modulated by choosing different frequencies of an applied electric field. Specifically, at high frequencies,

$$\mathrm{Re}\left[\underline{f}_{\mathrm{CM}}(\omega \to \infty)\right] \approx \frac{\varepsilon_p - \varepsilon_m}{\varepsilon_p + 2\varepsilon_m}, \tag{2a}$$

On the other hand, at low frequencies (i.e., from 0 [DC field] to about 10 kHz),

$$\mathrm{Re}\left[\underline{f}_{\mathrm{CM}}(\omega \to 0)\right] \approx \frac{\sigma_p - \sigma_m}{\sigma_p + 2\sigma_m}. \tag{2b}$$

For a submicron or micron-sized particle, the particle conductivity σ_p is due to both the particle bulk conductivity ($\sigma_{p,\mathrm{bulk}}$) and the particle surface conductivity ($2Ks/a$), and is given by

$$\sigma_p = \sigma_{p,\mathrm{bulk}} + 2Ks/a, \tag{3}$$

where Ks is the surface conductance ranging from 0.2 to 2.1 nS [36, 37], and $\sigma_{p,\mathrm{bulk}}$ is nearly zero for polystyrene dielectric particles.

Eq. (1) suggests that the separation of the same type of particles can be achieved based on particle size because the DEP force for a spherical particle is scaled to the cubic power of particle radius. Furthermore, examination of Eq. (2b) and Eq. (3) suggests a possible separation of particles based on different DEP polarities. It is also noted from Eq. (3) that for a given medium, the particle conductivity increases with decreasing particle size. Thus at low frequencies, Eq. (2b) indicates that through appropriately choosing the conductivity of suspending medium, one can ensure that smaller particles experience pDEP and larger particles experience nDEP.

2.2 Device design and separation principle

The present microfluidic device is a modified H-filter with insulating blocks, and its microstructures and dimensions are schematically illustrated in Fig. 1A. Such a modified H-filter device was fabricated using PDMS, and the fabrication follows standard photo- and soft-lithography protocols with details described elsewhere [27]. The device consists of the inlet A to introduce test samples containing a mixture of particles with three different sizes (termed as small, medium, and large thereafter), the inlet B to introduce a buffer solution for generating hydrodynamic focusing effect, the outlet C to collect large particles experiencing nDEP, the outlet D to collect medium particles experiencing nDEP, and the outlet E to collect small particles experiencing pDEP. Except for the

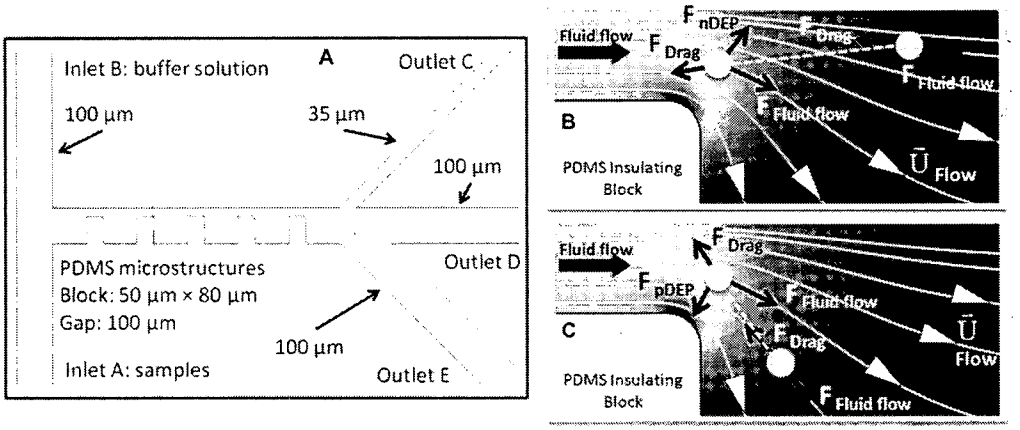

Figure 1. (A) Schematic diagram showing the microstructures and dimensions of a modified H-filter with multiple outlet channels for separation of multiple particles. (B–C) Force diagram, electric field distribution, fluid flow streamlines near an insulating block corner where a particle experiences a hydrodynamic drag force and a repulsive nDEP force as shown in (B) or an attractive pDEP force as shown in (C).

outlet channel C having 35 μm width, other inlet and outlet channels are 100 μm wide. The choice of smaller channel width for the outlet channel C than that for the outlet channel D is to prevent the medium particles from entering to the outlet C. All inlet and outlet channels are connected to their respective reservoirs of 5 mm in diameter. Of a particular note is the inclusion of five PDMS blocks aligned along one side of a 100 μm wide main channel, and each block has 50 μm width and 80 μm height and is separated by a 100 μm wide gap. As will be discussed in Section 3, the choice of these insulating block dimensions is based on the numerical simulation results using COMSOL Multiphysics software.

The device is used for the separation of multiple particles by utilizing DEP forces that are present near the corners of the insulating blocks. For a particle traveling near an insulating block corner, electric field distribution, fluid flow streamlines, and physical forces exerting on the particle experiencing nDEP and pDEP are shown in Fig. 1B and C, respectively. In the absence of an electric field, the particle moves following the flow streamline. When an electrical voltage is imposed through the reservoirs of the inlet and outlet channels, the presence of insulating blocks causes variations of electrical current density that induce nonuniform electric fields, giving rise to DEP forces. A repulsive nDEP force causes the particle to move away from the corner (Fig. 1B), and an attractive pDEP force draws the particle to move close to the corner (Fig. 1C). As a result, separation of particles can be achieved according to different magnitudes and kinds of the DEP forces. In particular, large particles experiencing stronger nDEP will move into the outlet channel C, medium particles experiencing weaker nDEP will move into the outlet channel D, and small particles experiencing pDEP will move into the outlet channel E. Based on this separation principle, it is clear that increasing the number of insulating blocks can lead to better particle separation.

2.3 Sample preparation and experimental setup

Two micrometer fluorescent polystyrene particles and 5 and 10 μm polystyrene particles (Duke Scientific, USA) suspended in a 13 μs/cm $NaHCO_3$ buffer solution were used in experiment. To prepare the sample suspension, 0.02 mL of 2 μm fluorescent polystyrene particles (of 1% solids original concentration in DI water), 1 mL of 5 μm polystyrene particles (10^7/mL in DI water) and 2 mL of 10 μm polystyrene particles (10^6/mL in DI water) were added in a microcentrifuge tube. The particle mixture was first centrifuged at 13 300 rpm for 3 min and then transferred into 1 mL $NaHCO_3$ buffer solution with its conductivity of 13 μs/cm.

Prior to separation experiment, the fabricated PDMS microchannels were thoroughly flushed with a 13 μs/cm $NaHCO_3$ solution for three times, and then the sample suspension was injected via the inlet channel A. After platinum electrodes were placed in both inlet and outlet reservoirs, the $NaHCO_3$ buffer solution was withdrawn from outlets to produce suction effects that induced a pressure-driven flow for a desired particle velocity. Subsequently, the liquid level at two reservoirs was balanced so that the symmetric hydrodynamic focusing was realized at the entrance T junction (Fig. 4A). The 5 mm reservoirs were experimentally proved to allow for such steady flow to last for 5 min. AC voltages were produced from a function generator (Agilent 33250A) and were amplified by a customized high AC voltage amplifier (Optrobio, Singapore). The generated sinusoidal wave monitored by an oscilloscope (CombiScope® HM 1008, USA).

3 Results and discussion

3.1 Numerical simulation results

As shown in Eq. (1), the magnitude of DEP force is proportional to the gradient of the square of electric field. Numerical simulations using the finite-element-based COMSOL Multiphysics software were performed to obtain the electric field distribution, flow streamlines as well as the gradient of the square of electric field (the last can be used to represent the magnitude of DEP force). Specially, the effects of block gap and width on the magnitude of DEP force were examined, and the resultant optimal geometric dimensions of a block were adopted in the device design used in experiment.

In the simulations, the thin electric double layer assumption was used such that the electric field distribution is governed by Laplace's equation. Referred to Fig. 1A, two boundary conditions include: (i) a specified AC voltage of 635 V is applied at both inlets A and B while the outlets C, D, and E are electrically grounded, and (ii) the electric field components normal to insulating walls and blocks must vanish. Based on the low Reynolds number (Re $\ll$ 0.1), the flow field is governed by Stokes's equation with the boundary conditions comprising no-slip velocity on channel walls and blocks, an inflow velocity of 100 μm/s at two inlets, and atmospheric pressure at three outlets.

3.2 Effect of the block gap

To understand the effect of the block gap on electric field distribution and DEP force characteristics, simulations were performed with a 100 μm wide microchannel consisting of two adjacent insulating blocks (50 μm wide × 80 μm high), with the block gap varied from 25 μm (Fig. 2A) to 100 μm (Fig. 2B). The simulated electric field distribution shows that in all cases, electric field intensity is high at the constrictions between the blocks and the wall with the local electric field maxima at the corners, but the intensity shows significantly lower at surrounding areas.

When a 25 μm wide gap is designed, the insulating blocks are located too closely (Fig. 2A). The electric field intensity at the top portion of the block gap sandwiched by two constrictions becomes relatively high due to the surrounding high field intensities produced by the two constrictions as compared to the case of the 100 μm wide gap (Fig. 2B). This spatial difference in such electric field intensities across the block gap (along the vertical direction) leads to an unwanted nDEP force which pushes the particle downwards and reduces the wanted nDEP force effects induced at the block corners as schematically illustrated in Fig. 2A. To support this simulation interpretation, the *y*-component nDEP force is analyzed by computing the *y*-component gradient of the square of the electric field ($\nabla_y|\vec{E}|^2$) along the *x* direction from the center of the first block to that of the second block (as labeled by **a** and **a'** in Fig. 2A). In Fig. 2C, for the 25 μm wide gap, $\nabla_y|\vec{E}|^2$ expectedly reaches its highest values at the

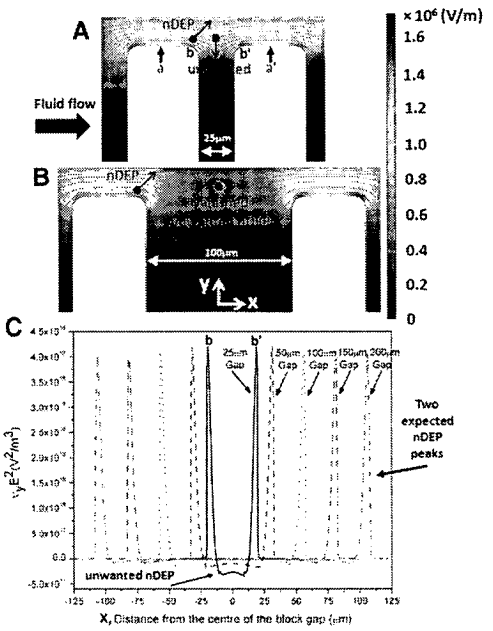

Figure 2. (A–B) Simulation results of electric field distribution and fluid streamlines near two 50 μm wide insulating blocks spaced (A) 25 μm and (B) 100 μm apart. The *y*-component gradient of the square of electric field representing nDEP force (from the center of the first block and that of second block as labeled by **a** and **a'** in A) (C) for the block gap of 25, 50, 100, 150, and 200 μm. It is noted that the nDEP force arrows in A and B are not drawn in scale.

right corner of the first block and the left corner of the second block (as labeled by **b** and **b'**), implying dominant nDEP forces for particle separation. However, the negative value of $\nabla_y|\vec{E}|^2$ occurs at the block gap and it can be interpreted as the downwards nDEP force which is unfavorable for the separation. On the other hand, the negative values of $\nabla_y|\vec{E}|^2$ gradually and completely disappear for the wider gap of 50 and 100 μm, respectively. These results suggest that at 100 μm, the gap becomes as wide as the main channel, and therefore the electric field has enough spaces to fully re-distribute after compressed in the constriction. Hence, the electric field intensity at the block gap is negligible and the negative value of $\nabla_y|\vec{E}|^2$ is not present. It is also found that in comparison with the 100 μm wide gap, the channel with 25 μm wide gap creates the substantial negative value of $\nabla_y|\vec{E}|^2$ up to 158% although a slight increase in the maximum value of $\nabla_y|\vec{E}|^2$ of about 2.4% is noted. Furthermore, as the block gap increases more than the main channel width (> 100 μm), no noticeable change of $\nabla_y|\vec{E}|^2$ can be observed. Therefore, from the simulation results, it is recommended that to avoid the unwanted DEP force, the block gap should be as wide as the main channel.

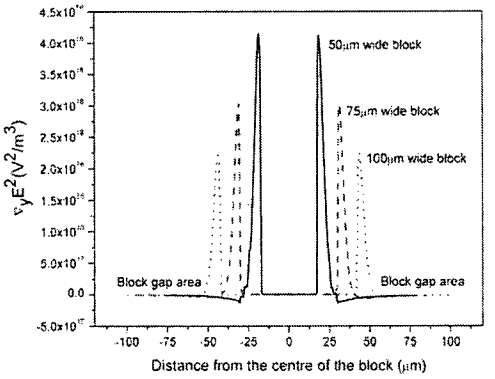

Figure 3. The y-component gradient of the square of electric field for three different block widths of 50, 75, and 100 μm with a fixed block gap of 100 μm.

3.3 Effect of the insulating block width

The effect of insulating block width on the magnitude of DEP forces is examined by computing the value of $\nabla_y|\vec{E}|^2$ in the case of three different block widths of 50, 75, and 100 μm while keeping a fixed block gap of 100 μm. The simulation results in Fig. 3 show that the smallest (50 μm wide) insulating blocks produce the highest value of $\nabla_y|\vec{E}|^2$ at the block corners as compared to other cases. In this case, the electric fields around the smaller blocks vary more rapidly, thus increasing higher electric field gradients as compared to those around the larger blocks. In addition, it is important to note that the block width has no effect on the negative value of $\nabla_y|\vec{E}|^2$ at the block gap area as long as the block gap is as wide as the main channel. Hence, based on the simulation results of the effects of block gap and width, the design guidelines can be established that the optimal gap width should be the same as the main channel width, and smaller insulating blocks are recommended to enhance DEP force effects for maximum lateral deflection of particle motion and thus higher efficient particle separation, although subject to the soft lithography limitation at about 20 μm.

3.4 Separation of multiple particles by nDEP and pDEP

According to the design guidelines presented above, the fabricated device consists of five insulating blocks (50 μm wide × 80 μm high) which are spaced 100 μm apart in a 100 μm wide microchannel (Fig. 4A). The 50 μm wide blocks were chosen because fabrication of smaller blocks could be more troublesome to maintain a rectangular shape. To demonstrate the separation of multiple particles by nDEP and pDEP, 2 μm fluorescent polystyrene particles and bare (nonfluorescent) 5 and 10 μm polystyrene particles were selected. Although these particles are made of polystyrene, they possess different electrical conductivities according to the size-dependent surface conductivity term in the CM factor as shown in Eq. (2) and Eq. (3). Therefore, in a sufficiently dilute buffer solution, smaller particles could be more conductive than the suspending medium and would experience an attractive pDEP force while the larger particles became less conductive than the medium and will undergo repulsive nDEP forces.

To achieve such manipulation, a suitable buffer solution was determined. We first conducted experiments by observing DEP motions of all particle sizes near insulating blocks to decide whether they were attracted to or repelled from the block corners under an AC voltage of 635 V at 5 kHz in a stagnant buffer solution. The buffer solution conductivities ranging from 13 to 80 μS/cm were tested. Experimental results show that a 13 μS/cm solution provided desirable DEP conditions such that 2 μm fluorescent particles experienced an attractive pDEP force and thus moved to the corners while 5 and 10 μm particles were repelled from the corners by repulsive nDEP forces. For the medium conductivity of 80 μS/cm, only particle motion under nDEP was observed for all particle sizes. These experimental observations are consistent with the theoretical DEP behaviors predicted by the CM factor which is based on the surface conductance of 1.3 nS for microparticles larger than 1 μm in diameter [17]. In particular, for the 13 μS/cm $NaHCO_3$ buffer solution, the calculated values of the CM factor for 2, 5, and 10 μm particles as shown in Eq. (1) together with Eq. (3) are +0.25, −0.07, and −0.25 at 5 kHz, respectively. Moreover, Supporting Information Fig. 1 shows the plot of CM factor versus electric field frequency varied from 1 kHz to 100 MHz, which gives the crossover frequency of 0.42 MHz for 2 μm particles where the other two particle sizes have no crossover frequency (see Supporting Information).

Figure 4 demonstrates particle transport, focusing, and separation of multiple particles by nDEP and pDEP in a 13 μS/cm $NaHCO_3$ buffer solution under a continuous pressure-driven flow. In Fig. 4A, a mixture of multiple particles introduced from the lower inlet A was hydrodynamically focused by the flow from the upper inlet B at an entrance T junction. As a result, the flowing particles could be confined near insulating block corners where strong DEP forces are present. In the absence of any applied AC voltage, all particles experienced only hydrodynamic drag forces and thus randomly moved to the lower outlet E and the middle outlet D as presented in Fig. 4B. By applying a sufficient (or threshold) AC voltage of 635 V_{AC} at 5 kHz, it was observed that good separation of multiple particles was successfully achieved as shown in Fig. 4C. The equivalent electric field is 635 V/cm with the channel length of 1 cm. The separation phenomenon can be explained as followed. According to Eq. (1), since the magnitude of a DEP force is scaled to the cubic power of particle radius, the 10 μm particles experienced a more dominant repulsive nDEP force and hence were repelled to the upper outlet C while the 5 μm particles were deflected to the outlet D with a weaker nDEP force. Meanwhile, 2 μm fluorescent particles were fractionated by a pDEP force into the outlet

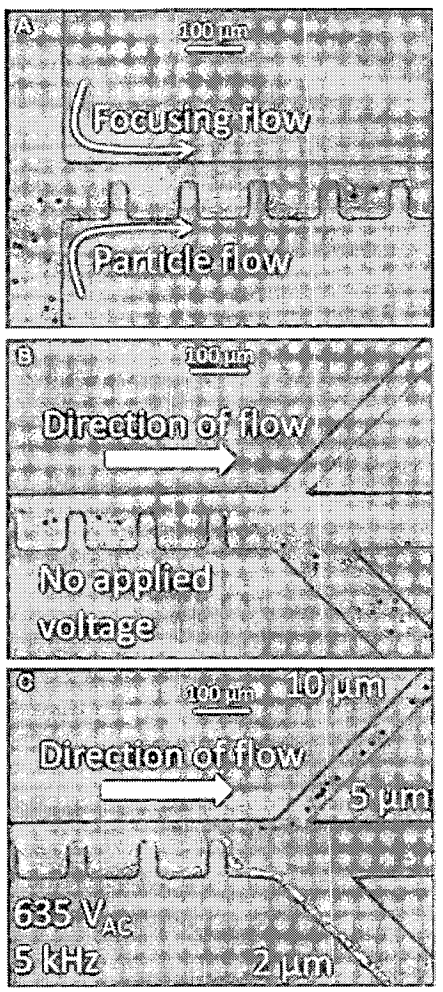

Figure 4. (A) Particle transport and focusing by two-stream pressure-driven flows at an entrance T junction. (B) The focused particle stream in the absence of an applied AC voltage near the three-outlet exit region. (C) Continuous separation of 2 μm fluorescent particles by an attractive pDEP force and both 5 and 10 μm particles by a repulsive nDEP force due to their different sizes under 635 V_{AC} at 5 kHz in a 13 μs/cm $NaHCO_3$ buffer solution.

E. The experiments were repeated three times, and each lasted for 3 min. The separation efficiency for all particle sizes is of 99% in all experiments (see a movie in Supporting Information). The particle velocity varies in a range of 200–1000 μm/s in the main channel and the constrictions. The average velocity of particles traveling through the block area is about 600 μm/s. As the insulating block area is 850 μm long, the separation time window is approximately 1.4 s.

Furthermore, it is known that Joule heating could be an issue that can cause temperature rise and thus potentially affect the performance of iDEP-based microfluidic devices. However, we did not observe any noticeable Joule heating effects in our experiment. In our case involving an applied electric field of 635 V/cm and a medium conductivity of 13 μs/cm, the Joule heating ($\sigma_{medium}E^2$) can be estimated to be about 5 MW/m^3. According to Sridharan et al. [38] who studied Joule heating effects on electrothermal flow near the corners of insulating blocks in a glass/PDMS microchannel, even with Joule heating of 19 MW/m^3 at 1 kHz, which is ~3.8 times higher than our case, the local temperature rise was computed to be less than 5 K, suggesting negligible Joule heating effects.

4 Concluding remarks

This work has presented a new application of the modified H-filter with optimal insulating PDMS blocks for continuous separation of multiple particles using nDEP and pDEP. Under an applied voltage of 635 V_{AC} at 5 kHz, the device performance is demonstrated by separating a three-sized particle mixture, including 2 μm fluorescent particles with an attractive DEP force and both 5 and 10 μm nonfluorescent particles with differential repulsive DEP forces. The reported separation efficiency of 99% has evidently proved the device performance to be promising to deal with multicomponent biosamples. The conducted simulation analyses taking into consideration of the effects of insulating block gap and width on electric field distribution and DEP force characteristics essentially leads to recommended design guidelines for the optimal geometric dimensions. Thus, these guidelines can also be considered as the criteria in designing other DC- and AC-iDEP devices using insulating blocks as constrictions for chemical and biomedical applications.

The authors gratefully acknowledge the research grant (AcRF RG17/05) from the Ministry of Education of Singapore to C.Y. and the Ph.D. Scholarship from Nanyang Technological University to N.L.

The authors have declared no conflict of interest.

5 References

[1] Lewpiriyawong, N., Yang, C., in: Wang, L. (Ed.), *Advances in Transport Phenomena 2011*, Springer International Publishing, Switzerland 2014, pp. 29–62.

[2] Choi, S., Park, J.-K., *Lab Chip.* 2005, *5*, 1161–1167.

[3] Yang, F., Yang, X., Jiang, H., Bulkhaults, P., Wood, P., Hrushesky, W., Wang, G., *Biomicrofluidics* 2010, *4*, 013204.

[4] Wang, L., Lu, J., Marchenko, S. A., Monuki, E. S., Flanagan, L. A., Lee, A. P., *Electrophoresis* 2009, *30*, 782–791.

[5] Cetin, B., Kang, Y., Wu, Z., Li, D., *Electrophoresis* 2009, *30*, 766–772.

[6] Kang, Y., Cetin, B., Wu, Z., Li, D., *Electrochim. Acta* 2009, *54*, 1715–1720.

[7] Iliescu, C., Xu, G. L., Samper, V., Tay, F. E. H., *J. Micromech. Microeng.* 2005, *15*, 494–500.

[8] Yu, L., Iliescu, C., Xu, G., Tay, F. E. H., *J. Microelectromech. Syst.* 2007, *16*, 1120–1129.

[9] Iliescu, C., Tresset, G., Xu, G., *Appl. Phys. Lett.* 2007, *90*, 234104.

[10] Wang, C., Jia, G., Taherabadi, Madou, L. H., *J. MEMS* 2005, *14*, 348–358.

[11] Park, B. Y., Madou, M. J., *Electrophoresis* 2005, *26*, 3745–3757.

[12] Braschler, T., Demierre, N., Nascimento, E., Silva, T., Oliva, A. G., Renaud, P., *Lap Chip* 2008, *8*, 280–286.

[13] Lewpiriyawong, N., Yang, C., *Biomicrofluidics* 2012, *6*, 012807.

[14] Lewpiriyawong, N., Kandaswamy, K., Yang, C., Ivanov, V., Stocker, R., *Anal. Chem.* 2011, *83*, 9579–9585.

[15] Lewpiriyawong, N., Yang, C., Lam, Y. C., *Electrophoresis* 2010, *31*, 2622–2631.

[16] Li, S., Li, M., Hui, Y., Sanna., Cao, W., Li, W., Wen, W., *Microfluid. Nanofluid.* 2013, *14*, 499–508.

[17] Li, M., Li, S., Cao, W., Li, W., Wen, W., Alici, G., *Microfluid. Nanofluid.* 2013, *14*, 527–539.

[18] Cummings, E. B., Singh, A. K., *Analyt. Chem.* 2003, *75*, 4724–4731.

[19] Kang, K. H., Kang, Y., Xuan, X., Li, D., *Electrophoresis* 2006, *27*, 694–702.

[20] Zhu, J., Tzeng, T., Xuan, X., *Electrophoresis* 2010, *31*, 1382–1388.

[21] Church, C., Zhu, J., Xuan, X., *Electrophoresis* 2011, *32*, 527–531.

[22] Pysher, M. D., Hayes, M. A., *Anal. Chem.* 2007, *79*, 4552–4557.

[23] Lapizco-Encinas, B. H., Simmons, B. A., Cummings, E. B., Fintschenko, Y., *Electrophoresis* 2004, *25*, 1695–1704.

[24] Barrett, L. M., Skulan, A. J., Singh, A. K., Cummings, E. B., Fiechtner, G. J., *Anal. Chem.* 2005, *77*, 6798–6804.

[25] Lapizco-Encinas, B. H., Ozuna-Chacón, S., Rito-Palomares, M., *J. Chromatogr. A* 2008, *1206*, 45–51.

[26] Hawkins, B. G., Smith, A. E., Syed, Y. A., Kirby, B. J., *Anal. Chem.* 2007, *79*, 7291–7300.

[27] Lewpiriyawong, N., Yang, C., Lam, Y. C., *Biomicrofluidics* 2008, *2*, 034105.

[28] Zhu, J., Xuan, X., *Electrophoresis* 2009, *30*, 2668–2675.

[29] Church, C., Zhu, J., Nieto, J., Keten, G., Ibarra, E., Xuan, X., *J. Micromech. Microeng.* 2010, *20*, 065011.

[30] Kim, U., Qian, J., Kenrick, S. A., Daugherty, P. S., Soh, H. T., *Anal. Chem.* 2008, *80*, 8656–8661.

[31] Srivastava, S. K., Gencoglu, A., Minerick, A. R., *Anal. Bioanal. Chem.* 2011, *399*, 301–321.

[32] Srivastava, S. K., Baylon-Cardiel, J. L., Lapizco-Encinas, B. H., Minerick, A. R., *J. Chromatogr. A.* 2011, *1218*, 1780–1789.

[33] Zhang, L., Tatar, F., Turmezei, P., Bastemeijer, J., Mollinger, J. R., Piciu, O., Bossche, A., *J. Phys.* 2006, *34*, 527–532.

[34] Brody, J. P., Yager, P. *Sensors Actuat.* 1997, *58*, 13–25.

[35] Pohl, H. A., *Dielectrophoresis-The Behavior of Neutral Matter in Nonuniform Electric Fields*, Cambridge University Press, Cambridge (UK) 1978.

[36] Morgan, H., Green, N. G., *AC Electrokinetics: Colloids and Nanoparticles*, Research Studies Press, Philadelphia 2002.

[37] Arnold, W. M., Schwan, H. P., Zimmermann, U., *J. Phys. Chem.* 1987, *91*, 5093–5098.

[38] Sridharan, S., Zhu, J., Hu, G., Xuan, X., *Electrophoresis* 2011, *32*, 2274–2281.

